Effects of global MHD instability on operational high beta-regime in LHD

K.Y.Watanabe 1), S.Sakakibara 1), Y.Narushima 1), H.Funaba 1), K.Narihara 1), K.Tanaka 1), T.Yamaguchi 2), K.Toi 1), S.Ohdachi 1), O.Kaneko 1), H.Yamada 1), Y.Suzuki 3), W.A.Cooper4), S.Murakami 5), N.Nakajima 1), I. Yamada 1), K.Kawahata 1), T.Tokuzawa 1), A.Komori 1) and LHD experimental group

1) National Institute for Fusion Science, 322-6 Oroshi, Toki, 509-5292, Japan
2) The Graduate University for Advanced Studies, Toki 509-5292, Japan
3) Graduate School of Energy Science, Kyoto Univ., Kyoto, 606-8224, Japan
4) Centre de Recherches en Physique des Plasmas, Association Euratom / Confederation Suisse, EPFL, 1015 Lausanne, Switzerland
5) Department of Nuclear Engineering, Kyoto Univ., Kyoto 606-8501, Japan

e-mail contact of main author: kiyowata@LHD.nifs.ac.jp

Abstract. In the Large Helical device (LHD), the operational highest averaged beta value has been expanded from 3.2% to 4% in last two years by increasing the heating capability and exploring a new magnetic configuration with a high aspect ratio. Although the MHD stability properties are considered to be unfavourable in the new high aspect configuration, the heating efficiency due to neutral beams and the transport properties are expected to be favourable in a high beta range. In order to make clear the effect of the global ideal MHD unstable mode on the operational regimes in helical systems, specially the beta gradients in the peripheral region and the beta value, the MHD analysis and the transport analysis are done in a high beta range up to 4% in LHD. In a high beta range of more than 3%, the maxima of the observed thermal pressure gradients in the peripheral region are marginally stable to a global ideal MHD instability. Though a gradual degradation of the local transport in the region has been observed as beta increases, a disruptive degradation of the local transport does not appear in the beta range up to 4%.

1. Introduction

A Heliotron device is a probable candidate of toroidal magnetic confinement systems as thermonuclear fusion reactor under steady-state operation because it can confine plasma with only external coils and install a well-defined divertor configuration. However, it is theoretically predicted that it has a disadvantage with respect to pressure driven magneto-hydrodynamics (MHD) instabilities [1]. Ideal MHD instabilities have a possibility to strongly limit the operational regime of the plasma parameters such as beta, pressure gradient and/or so on. In tokamaks, it is well known that the operational beta limits are quite consistent with theoretical predictions of ideal linear MHD theory [2]. On the contrary, in helical plasmas, a limited number of systematic studies about the effect of pressure driven ideal MHD instabilities on the operational beta range in experiments have been reported, for examples, on Heliotron DR [3], the compact helical system (CHS) [4] and the Large Helical Device (LHD) [5,6]. In the recent papers on LHD [5,6], the relationships between the unstable condition of the pressure driven MHD modes and the experimentally observed pressure gradients at some resonant rational surfaces based on the consistent MHD equilibrium with the measured plasma parameters data like the plasma stored energy, toroidal current, electron density and temperature profiles, which are enabled by powerful profile measurement systems, have been reported. According to them, the pressure gradients in the core region (a normalized minor radius, $\rho \sim 0.5$) are governed by the ideal global MHD instability driven by pressure gradients. When a growth rate of the low-n ideal MHD unstable mode is applied as an index of the criteria, the pressure gradients do not exceed it. However, we have not obtained any conclusive results on the effects of the ideal global MHD instability in the peripheral region

(ρ~0.9) on the operational regimes because the achieved beta values have not been high enough to reach a clear conclusion about this. Generally speaking, in heliotron devices, the global MHD mode in the core region is unstable in the intermediate beta range and it is stable in the high beta range. On the other hand, because the instability in the peripheral region is more unstable as the beta becomes higher, it is considered that the behaviour of the instability in the peripheral region limits the operational beta range, and it should be studied systematically.

MHD studies from the other aspects of the above have been done in previous LHD experiments as the followings. With regard to the MHD fluctuations with the resonance in the core region, stabilization due to spontaneous generation of magnetic well has been verified in the experiment [7]. MHD modes excited in the edge region have been observed even in the low-β regime, and amplitudes of edge resonant modes such as m/n=2/3 mode are considerably enhanced in the H-mode plasma with steep edge pressure gradient [8]. A disruptive degradation of an improvement factor of the global energy confinement time had not been observed up to $<\beta_{dia}>$ ~3% [5,9].

Recently the increase of heating capability and a new magnetic configuration with a high aspect ratio by changing the pitch parameter of helical coil, γ, enables exploration of the operational beta range up to 4% in LHD. LHD is a Heliotron device (poloidal period number L=2, and toroidal period number M=10) with a major radius of R_{ax}=3.5-4.1 m, an averaged minor radius of 0.6 m, magnetic field, B_t, up to 3T, and heating neutral beam with negative ion with beam energy of 150-180keV. The new configuration with higher aspect ratio (γ=1.22) is characterized by a smaller volume and smaller Shafranov shift than the so-called standard configuration (γ=1.254). Although the MHD stability properties are expected even worse theoretically in this configuration (γ=1.22) than the standard configuration because the magnetic well formation due to small Shafranov shift in a high beta range is reduced, the small shift is considered to contribute to the central deposition of neutral beam and hence the reduction of the direct loss of the beam by keeping the magnetic axis close to the tangential radius of the neutral beam in a high beta range. Moreover, the small volume is favourable for the extension of the operational density range according to a density limit empirical scaling, and the MHD equilibrium properties are favourable because of the small shift. Figure 1 shows the improvement factor (H_{ISS}) of the global energy confinement time on the ISS95 (International Stellarator Scaling 1995) empirical scaling [10] in the new high aspect configuration as a function of $<\beta_{dia}>$. Here $H_{ISS\text{-}diamag}$ and $H_{ISS\text{-}kin}$ are based on the diamagnetic flux measurement and the electron temperature and density profile measurements under the assumption of Z_{eff}=1 and T_i=T_e, respectively. The $<\beta_{dia}>$ is the diamagnetic beta value defined as $(2W_{dia}/3V_{p0})/(B_{av0}^2/2\mu_0)$, where W_{dia} is the diamagnetic energy. The B_{av0} and V_{p0} are averaged toroidal magnetic field inside the plasma boundary and plasma volume, respectively, and both of them are estimated under vacuum conditions. A disruptive degradation of both global energy confinement times based on the diamagnetic flux measurement and the profile measurements have not been observed up to $<\beta_{dia}>$ ~4%. However, the enhancement factors are gradually reduced as beta increases.

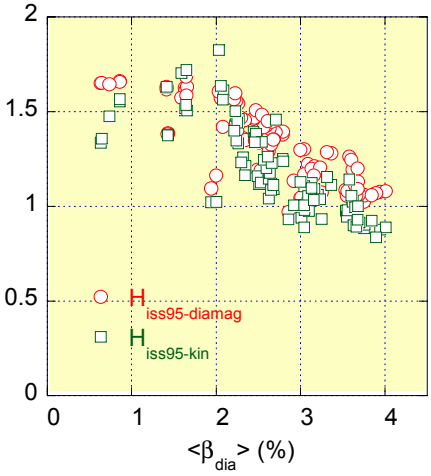

FIG.1 The improvement factor of effective energy confinement as a function of beta value.

In this paper, in order to study the role of ideal pressure driven MHD modes on the operational regime in LHD, especially in the peripheral region, we compare between the experimentally observed pressure gradients at peripherally located resonant rational surfaces and the theoretically predicted unstable region for ideal pressure driven MHD instabilities in the new high aspect configuration with R_{ax}=3.6m/γ =1.22, where the achieved beta value has been extended to 4%. And we study the relationships between the local transport property and the ideal MHD analysis results up to $<\beta_{dia}>$ ~4%. We also show the typical behaviour of the MHD property in the high aspect configuration.

2. Typical high-beta discharge and MHD analysis

Figure 2 shows typical MHD activities in high-beta discharge in the high aspect configuration with R_{ax}=3.6m/ γ=1.22. The B_t is set at 0.5 T. The $<\beta_{dia}>$ increases as the electron density increases. Three neutral beams are injected to this plasma and the deposition power is about 6.9 MW at 1.725s. At 1.74s the $<\beta_{dia}>$ reaches the maximum, $<\beta_{dia}>$~3.8%. At the time, $<\beta_{kin}>$ and $<\beta_{beam}>$ reach ~3.2% and ~1.0%, respectively. Here $<\beta_{kin}>$ and $<\beta_{beam}>$ are the thermal component and the beam component of the beta value, respectively. $<\beta_{kin}>$ is estimated twice as the electron beta gradients with an assumption of Z_{eff}=1 and T_i=T_e, where the electron temperature and density profiles are measured by Thomson scattering and FIR measurements, respectively. The beam pressure is estimated based on the Monte Carlo technique and the steady state Fokker-Plank solution [11]. It should be noted that the beam pressure is expected to be ~30% of the thermal pressure in LHD typical high beta discharges because the operational density range is relatively low (n_e <3x10^{19}m^{-3}) due to a low density limit, the electron temperature is relatively high as shown in Fig.3 and NB injected power is large. A drop of the $<\beta_{dia}>$ after 1.85s is due to the termination of a beam injector.

The m/n=1/1, 2/3 and 2/5 modes excited in the edge region are dominantly observed in this discharge. Here m and n are the poloidal and toroidal mode-numbers of the magnetic fluctuation, respectively. The m/n=1/1 and 2/3 modes grow from 0.7s and their amplitudes increase with $<\beta_{dia}>$. However,

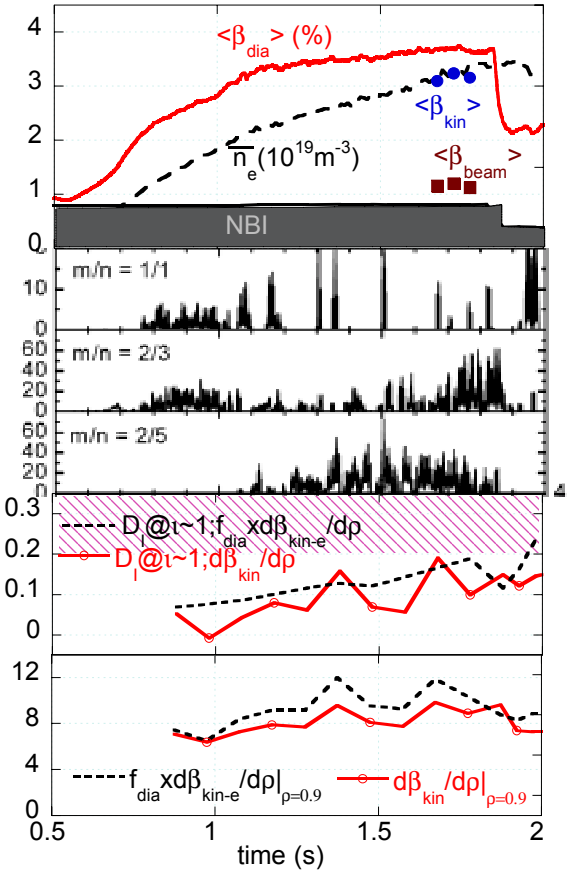

FIG.2 Temporal changes of plasma parameters in high-beta discharge.

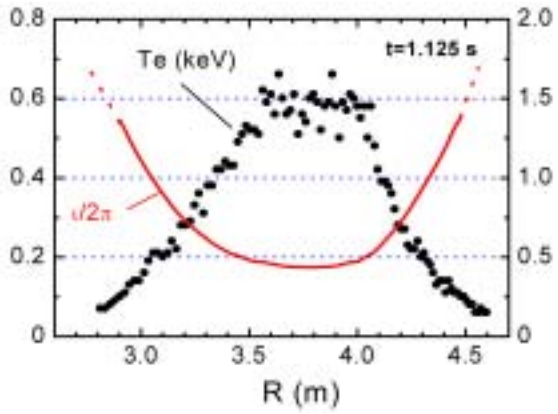

FIG.3 T_e and iota profiles at 1.125 s in Fig.2 discharge.

when $<\beta_{dia}>$ exceeds a certain value at 1 s, the m/n =1/1 mode is frequently interrupted and the amplitude of m/n=2/3 mode starts to decrease. Then $<\beta_{dia}>$ starts to increase suddenly, and the amplitude of the m/n=2/5 mode increases after that. At 1.75s, the degradation of $<\beta_{dia}>$ occurs with the growth of the m/n=2/3 mode and the reduction of the m/n=2/5 amplitude, although the heating and the supply of H_2 gas are still maintained. The bottom figure of Fig.2 shows the temporal changes of the thermal pressure gradient, $d\beta_{kin}/d\rho$ and the pressure gradient including the beam effect, $f_{dia}xd\beta_{kin\text{-}e}/d\rho$ around the m/n=1/1 resonant surface. Here we assume beam pressure gradients are proportional to the electron beta gradients, $d\beta_{kin\text{-}e}/d\rho$, and the sum of the thermal pressure and the beam pressure coincides with the stored plasma energy measured by the diamagnetic flux loop (f_{dia} is set to let $f_{dia}x<\beta_{kin\text{-}e}>$ is equal to $<\beta_{dia}>$). Both pressure gradients increase with $<\beta_{dia}>$. The $d\beta_{kin}/d\rho$ saturates at 1.1 s. After the m/n =1 mode is suppressed at 1.2s, the gradient increases again. The Mercier parameter D_I, which is well used as the index of high-n ideal stability, indicates the MHD mode is unstable because of the reduction of magnetic shear due to finite-beta effect. In this discharge, the low-n ideal mode is expected to be stable because the D_I is less than 0.2. Then, the observed m/n=1/1 mode is considered to be a resistive mode.

The equilibrium reconstruction is done for this discharge by the 3-D MHD equilibrium code VMEC [12], and T_e and rotational transform profiles are shown in Fig.3 as an example. The flattening structures of T_e profiles are found, for example, near the m/n=1/1 resonant surface. These asymmetrical structures are often observed in high-beta discharges, and however, it is difficult to apply such profiles to the present equilibrium reconstruction. This flattening may contributes the stabilization of the ideal and resistive modes. One of possibilities for the formation of the asymmetrical profile in periphery is due to variation of magnetic surfaces such as the growth of the intrinsic magnetic island due to an error field in finite beta plasmas [13].

Figure 4 shows changes of the amplitudes of observed MHD modes as a function of $<\beta_{dia}>$ in the $\gamma = 1.22$ configuration. Although the m/n=2/1 mode excited in core region has been observed in the $<\beta_{dia}>$ range of less than 2.5% in previous experiments, this mode disappears in the high-beta regime. The resonant surfaces with ι=1 are located at ρ~0.9 and their resonant modes are dominantly observed in the $<\beta_{dia}>$ range with more than 2.5%. While the amplitude of the m/n=1/1 mode increases with $<\beta_{dia}>$, it disappears or is intermittently observed when $<\beta_{dia}>$ exceeds 2.8%. Although the changes of the amplitudes of m/n=2/3 and 1/2 modes are similar to the

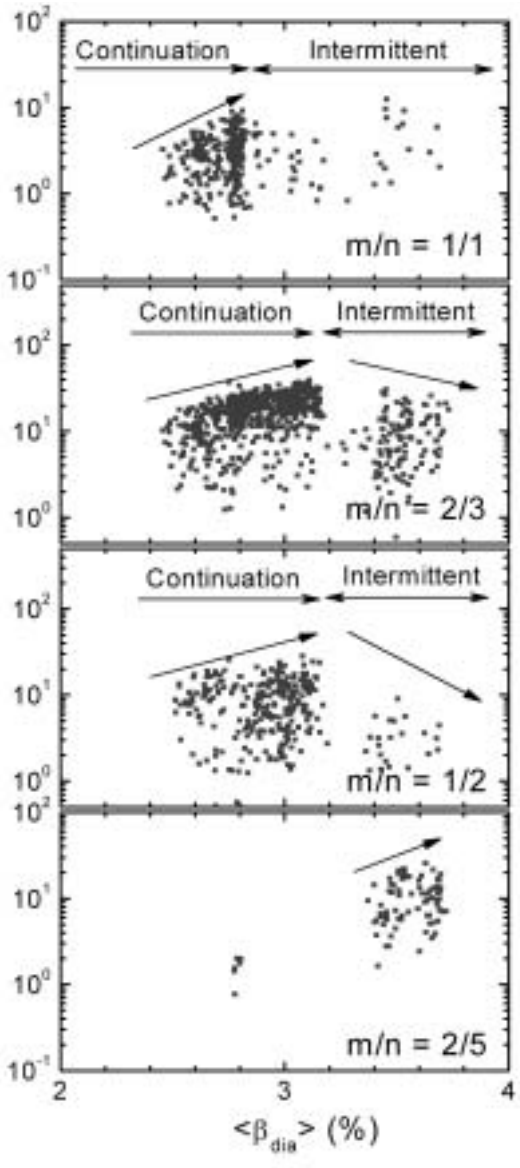

FIG.4 Beta dependence of MHD modes

case of the m/n=1/1 mode, the threshold $<\beta_{dia}>$ where the mode disappears is higher. The m/n=2/5 mode appears when $<\beta_{dia}>$ exceeds 3.4%, the amplitudes still increase with $<\beta_{dia}>$ in the present $<\beta_{dia}>$ range. These phenomena suggest that the stable region is expanded from the inner region to the outer one. The destabilization of the MHD mode just outside the "stable" region may be caused by the steep pressure gradient outside the profile flattening as shown in Fig.3.

3. Relationships between the prediction of linear MHD stability and the experiments

Here, we consider the effect of the global ideal MHD mode in the peripheral region on operational regimes. Figure 5 shows the experimentally observed beta gradients in the peripheral region (ρ=0.9, ι~1) in the high aspect configuration with R_{ax}=3.6m/γ =1.22 as a function of $<\beta_{dia}>$. The data were obtained in 0.45T to 1.75T operation. Symbols in Fig.5 correspond to the observed thermal beta gradients. Solid and dashed lines denote contours of the low-n (m/n =1/1) ideal MHD modes (with global mode structure) with $\gamma_{low\text{-}n}/\omega_A=10^{-2}$ and 5×10^{-3} for currentless equilibria. The growth rate is calculated with a MHD stability analysing code (TERPSICHORE [14]). Here $\omega_A=v_{A0}/R_0$, v_{A0} and R_0 are the Alfven velocity and the major radius at the magnetic axis. The dotted lines are the stability boundary of Mercier modes (with a highly localized mode structure / high-m limit) [15]. The observed beta gradients at ρ=0.9 increases with the beta up to $<\beta_{dia}>$=4%. The change of the gradients are observed around $<\beta_{dia}>$=1.5%, which corresponds to the Mercier unstable region. The envelope of the observed thermal pressure gradients in the beta range of $<\beta_{dia}>$=3-4% looks to coincide with a contour of the growth rate of the m/n=1/1 ideal MHD mode, $\gamma_{low\text{-}n}/\omega_A=10^{-2}$.

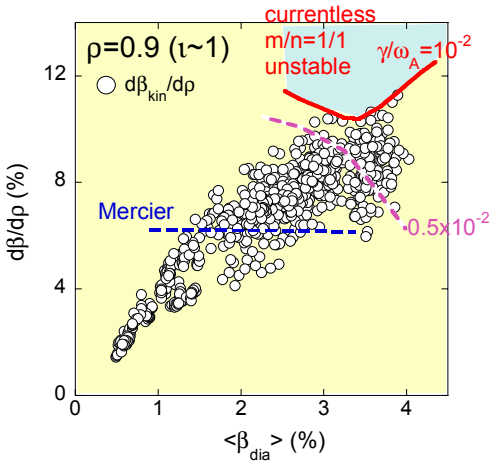

FIG.5 The observed thermal beta gradients at ρ=0.9 in $<\beta>$-$d\beta/d\rho$ diagram.

Now we consider the beam pressure effect on the global ideal MHD instability. According to a global ideal MHD stability analysis, the achieved thermal beta gradients are in a marginal stable region of the global MHD instability even around $<\beta_{dia}>$~4%. As shown in section 2, typical LHD high beta operations are done in low magnetic field and with high NBI power, where the beam pressure is fairly large. Figure 6 shows beta gradients including the beam component as a function of $<\beta_{dia}>$. Here we assume the beam pressure gradients are proportional to the electron beta gradients, and the sum of the thermal pressure and the beam pressure is the diamagnetic plasma energy as shown section 2. The other situations are the same as in Fig.5. The change of the beta gradients around $<\beta_{dia}>$=1.5% observed in Fig.5 almost disappears in Fig.6. The beta gradients including beam effects are in the unstable region of the low-n ideal MHD instability. Even where the

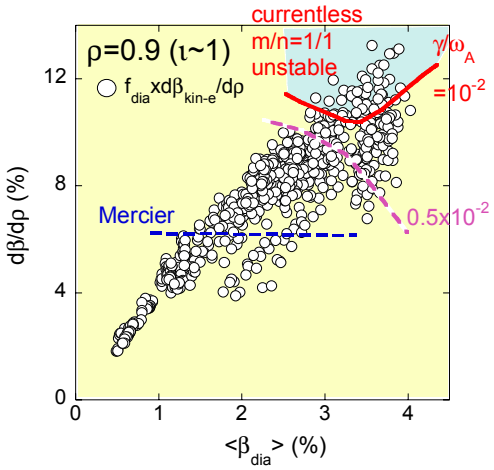

FIG.6 A beta gradient including a beam component at ρ=0.9 in $<\beta>$-$d\beta/d\rho$ diagram.

global ideal MHD mode is expected to be unstable, the beta gradients increase as the beta increases. These results suggest that either the beam pressure does not contribute the global ideal MHD instabilities or/and the beam pressure profiles may be broader that what is assumed here.

In order to know the effects of the beam component of the pressure on the ideal MHD mode, we need more detail information of the beam pressure. Moreover, we need larger heating power and/or the same kind of experimental study in a configuration with a higher aspect ratio. High heating power leads to high-density operation according to a density limit empirical scaling and/or the high magnetic field operation keeping the achieved beta value, where the contributions of the beam component on the total beta value are expected to be reduced. A configuration with a high aspect ratio is favourable from a viewpoint of the suppression of the loss of the NBI heating power in the high beta range, and its small volume leads to the extension of the operational density range. They also lead to the reduction of the contribution of the beam component.

4 Transport properties in high beta ranges

In order to analyse a local transport property in the peripheral region from a viewpoint of pressure gradients, we introduce a parameter, X, proportional to the heating power and inversely proportional to the beta gradient as follows,

$$X = Q_{\rho=0.9} \Big/ \left(-\frac{\partial \beta_{kin}}{\partial r}\bigg|_{\rho=0.9} S_{\rho=0.9} \frac{B^2}{2\mu_0} \right), \qquad (1)$$

where r is a minor radius, and $Q_{\rho=0.9}$ and $S_{\rho=0.9}$ are the heat flux due to input power at $\rho=0.9$ and an area of the $\rho=0.9$ magnetic surface, respectively. When a density is constant, the parameter coincides with the effective heat conductivity. Squares in Fig.7 show X normalized by a heat conductivity based on the so-called gyro-reduced Bohm model at $\rho=0.9$, as a function of $<\beta_{dia}>$. Circles show the beta gradients at $\rho=0.9$, which extracted from the data shown in Fig.5. The normalized X gradually increases with $<\beta_{dia}>$. The disruptive degradation of X is not observed around $<\beta_{dia}>$=3-4%, where the global ideal MHD modes is predicted to be marginally stable. However, the maxima of the normalized X suddenly increase when the beta gradients are in the Mercier unstable region, where resistive MHD modes are unstable and there is a possibility that the high-n ballooning mode is unstable. The effect of the resistive modes and the high-n ballooning modes on the transport properties is a future subject.

According to a local transport analysis, the local transport in the peripheral region is not seriously affected by the global ideal MHD modes around $<\beta_{dia}>$=3-4%. However, as shown in Fig.1, a gradual degradation of a global energy confinement on beta value is observed based on the ISS95 transport model. Figure 8 shows the electron density normalized by density limit proposed by Sudo et al. [16], H_{Sudo}, as a function of beta value. High beta discharges are done in a high collisionality range close to the density limit, H_{Sudo} >0.5 in $<\beta_{dia}>$ >2% and H_{Sudo} ~1 in $<\beta_{dia}>$ ~4%. According to a recent LHD transport scaling

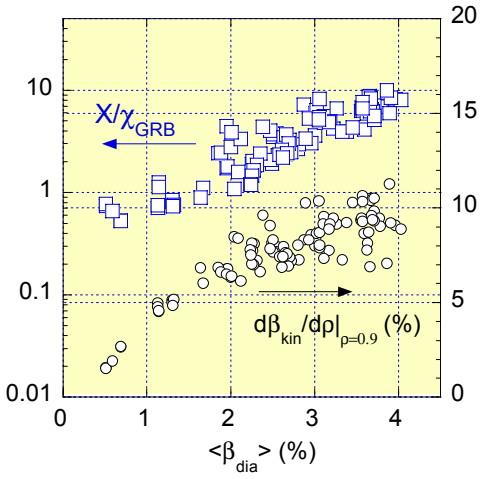

FIG.7 A normalized parameter, X at ρ=0.9 as a function of the beta value.

analysis in the high collisionality [17], the dependence of the global energy confinement time on the electron density changes from the ISS95 scaling, $\tau_E \sim n_e^{0.51}$ in the low collisionality range to $\tau_E \sim n_e^{0.28}$ in the high collisionality range. When we apply the new scaling law, a degradation of global energy confinement time is still observed. According to another scaling model, it is pointed out that the global confinement time scales according to the effective helical ripple of the magnetic field, $\varepsilon_{h\text{-}eff}$ [18]. In a high beta range, $\varepsilon_{h\text{-}eff}$ becomes larger than that in vacuum because of a Shafranov shift. The gradual degradation of global confinement time may follow this model. Moreover, it is reported that the broad heat deposition profile leads to the degradation of confinement time in LHD [19]. In low field operations, the heat deposition due to NBI is expected to be broad. This is another candidate of the explanation for the degradation of global energy confinement time.

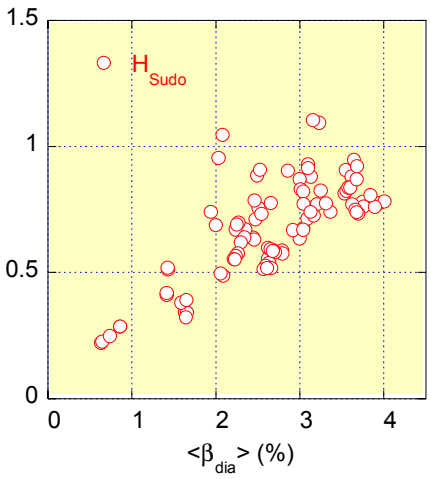

Fig.8 Electron density normalized by density limit proposed by Sudo et al.

5 Summary and discussion

In the Large Helical device (LHD), the operational highest averaged beta value has been expanded from 3.2% to 4% in last two years by increasing the heating capability and exploring a new magnetic configuration with a higher aspect ratio. Although the MHD stability properties are considered to be unfavourable in the new high aspect configuration, the heating efficiency due to neutral beam and the transport properties are expected to be favourable in the high beta range. In helical systems, in order to make clear the effect of the global ideal MHD unstable mode on the operational regimes, specially the beta gradients in the peripheral region and the total beta value, the MHD analysis and the transport analysis are done for the high beta operation up to $<\beta_{dia}>\sim 4\%$ in LHD. In a beta range of $<\beta_{dia}>=3\sim 4\%$, the global ideal MHD mode resonant with the peripheral rational surface, $\iota=1$, is marginal stable for the observed thermal component of beta gradients, that is, growth rates of a global ideal MHD mode are always below a value, $\gamma_{low\text{-}n}/\omega_A=10^{-2}$. However, the beta gradients including a beam component do not appear to be sensitive to the growth rates of a global ideal MHD mode. The beam pressure effect on the global ideal MHD instability is still unclear.

The local transport in the peripheral region and the global energy confinement are not seriously affected by the global ideal MHD instability around $<\beta_{dia}>=3\text{-}4\%$, where the global ideal MHD modes is expected unstable. The reason may be that the global ideal MHD instability around $<\beta_{dia}>=3\text{-}4\%$ is marginally stable. In order to make sure the effect of the global ideal MHD instability in the peripheral region on a local transport and a global energy confinement, we need larger heating power and/or the same kind of

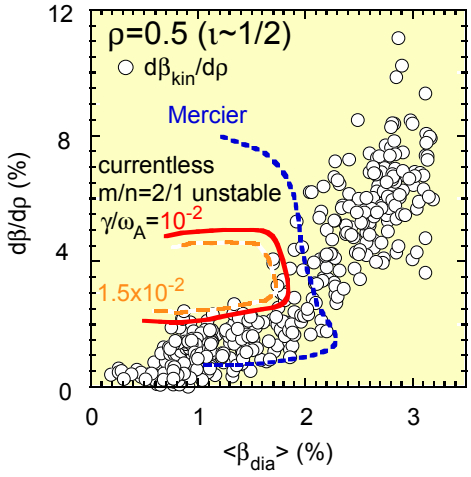

FIG.9 The observed thermal beta gradients at $\rho=0.9$ in $<\beta>$-$d\beta/d\rho$ diagram.

experimental study in a configuration with a higher aspect ratio.

Here we analyse the operational regimes based on a linear MHD theory. We know that the achieved pressure gradients are in the non-linear saturation phase. However, since it has not been clear how the pressure driven MHD instability affect the experimental operation regimes of the helical systems, our approach (evaluating the experimentally achievable pressure gradients by the linear growth rate and/or Mercier parameter) would be useful, because it could be a reference for more complicated non-linear analyses, and a criterion for a reactor design. Figure 9 shows the relationship between the experimentally observed thermal beta gradients in the core region (ρ=0.5, ι~1/2) and the theoretically predicted unstable region for ideal pressure driven MHD instabilities in the standard configuration with R_{ax} =3.6m/γ = 1.254 [5,6]. Symbols correspond to the observed thermal beta gradients. Solid and dashed lines denote contours of the low-n (m/n=2/1) ideal MHD modes with $\gamma_{low\text{-}n}/\omega_A=10^{-2}$ and $1.5\text{x}10^{-2}$ for currentless equilibria. In the core region, the maxima of the achieved pressure gradients seem to saturate against the contour of $\gamma_{low\text{-}n}/\omega_A= 1.5\text{x}10^{-2}$ in the range of $<\beta_{dia}>$ = 1~1.8%. When $<\beta_{dia}>$ exceeds ~1.8%, the maximum achieved pressure gradient more than doubles. Roughly speaking, $\gamma_{low\text{-}n}/\omega_A= 1\sim1.5\text{x}10^{-2}$ from the results of Figs.5 and 9 is considered a good index to determine the condition that the global ideal MHD instability limits the operational regime. For further verification, we need to extend the above comparative analyses between the experimental results and the theoretical prediction based on a linear theory to many magnetic configurations in LHD.

The authors deeply acknowledge the LHD experiment group for their great effort of LHD operation and maintenance.

References

[1] WAKATANI, M., NAKAMURA, Y., and ICHIGUCHI, K., Fusion Eng. Design 15 (1992) 395.
[2] ITER Physics Basis, Nuclear Fusion 39 (1999) 2137.
[3] YANAGI, N., et al., Nucl. Fusion 32 (1989) 1264.
[4] OKAMURA, S., et al, Nucl. Fusion 30 (1999) 1337.
[5] WATANABE, K.Y., et al, Fusion Sci. Tech. 46 (2004) 24.
[6] WATANABE, K.Y., et al, J. Plasma and Fusion Res. Ser, 6, (to be publised).
[7] SAKAKIBARA, S., Nucl. Fusion 41 (2001) 1177.
[8] TOI, K., et al., Nucl. Fusion 44 (2003) 217.
[9] YAMADA, H., et al., Plasma Phys. Control. Fusion 43 (2001) A55.
[10] STROTH, U., et al, Nuclear Fusion 36 (1996) 1063.
[11] HIRSHMAN, S.P., Phys. Fluids 26 (1983) 3553.
[12] NAGAYAMA, Y., et al., this conference.
[13] MURAKAMI, S., Nuclear Fusion 36 (1996) 359.
[14] COOPER, W. A., Plasma Phys. Control. Fusion 34 (1992) 1011.
[15] GRASSER, A.H., GREEN, J.M., and JOHNSON, J.L., Phys. Fluids 18 (1975) 143.
[16] SUDO, S., et al, Nucl. Fusion 30 (1990) 11.
[17] MIYAZAWA, J., et al, J. Plasma and Fusion Res. (to be submitted).
[18] YAMADA, H., et al., this conference.
[19] YAMADA, H., et al., Nucl. Fusion 43 (2003) 749.